



# Correlation of precipitate evolution with Vickers hardness in Haynes® 282® superalloy: *In-situ* high-energy SAXS/WAXS investigation

Sylvio Haas<sup>a,\*</sup>, Joel Andersson<sup>b</sup>, Martin Fisk<sup>c,d</sup>, Jun-Sang Park<sup>e</sup>, Ulrich Lienert<sup>a</sup>

<sup>a</sup> Photon Science, DESY, Hamburg, Germany

<sup>b</sup> Department of Engineering Science, University West, Trollhättan, Sweden

<sup>c</sup> Materials Science and Applied Mathematics, Malmö University, Malmö, Sweden

<sup>d</sup> Division of Solid Mechanics, Lund University, P.O. Box 118, SE-221 00 Lund, Sweden

<sup>e</sup> X-ray Science Division, Advanced Photon Source, Argonne National Laboratory, USA

## ARTICLE INFO

### Keywords:

X-ray analysis  
Characterization  
Hardness  
Nickel alloys  
SAXS  
WAXS

## ABSTRACT

The aim of this work is to characterize the precipitation kinetics in Haynes® 282® superalloys using *in-situ* high-energy Small Angle X-ray Scattering (SAXS) together with Wide Angle X-ray Scattering (WAXS). The phases identified by WAXS include  $\gamma$  (matrix),  $\gamma'$  (hardening precipitates), MC (metallic carbides), and  $M_{23}C_6/M_6C$  (secondary metallic carbides). The  $\gamma'$ -precipitates are spheroids with a diameter of several nanometres, depending on the temperature and ageing time. From the SAXS data, quantitative parameters such as volume fraction, number density and inter-particle distance were determined and correlated with *ex-situ* Vickers microhardness measurements. The strengthening components associated with precipitates and solid solutions are differentiated using the measured Vickers microhardness and SAXS model parameters. A square root dependence between strengthening attributable to the precipitates and the product of volume fraction and mean precipitate radius is found. The solid solution strengthening component correlates with the total volume fraction of precipitates.

## 1. Introduction

Superalloy possesses unique properties regarding strength and thermal stability at elevated temperatures. The excellent high-temperature properties are primarily associated with specific hardening phases that are present in these types of alloys. Such alloys typically find use in aero engines and land based turbines [1]. The most widely used superalloy in aero and land based turbines is Alloy 718, which comprises more than 50% of the superalloy usage today. It benefits from the  $\gamma''$  hardening phase, which has a stoichiometry  $Ni_3Nb$ . However, the strength reduces above approximately 650 °C, which is the service temperature limit of this alloy.

Alloys capable of withstanding higher temperature are needed to improve turbine efficiency. Alloys such as the newly developed Ni-based superalloy Haynes® 282® are now available. This alloy can withstand higher temperatures (approximately 800 °C) without significant loss in load-carrying ability [2–6]. Haynes® 282® contains smaller amounts of iron and niobium, but larger amounts of aluminium, titanium and molybdenum, making it a  $\gamma'$  hardening alloy while Alloy 718 is a  $\gamma''$  hardening alloy. The nominal compositions of Alloy 718 and

Haynes® 282® are given in the [Supplementary information](#).

Haynes® 282® was developed by Haynes International in 2005. The stoichiometry of the  $\gamma'$ -phase is nominally  $Ni_3(Al,Ti)$ , which nucleates in the matrix as spheroids [3]. Since the unique high temperature properties are governed by the nanometre sized  $\gamma'$ -phase, it is of great importance to understand the kinetics of precipitation. This is not only of importance when designing or optimizing the heat treatment of this and similar alloys, but is also of interest when processing the alloy or using it in various types of manufacturing processes [2,7–10]. The  $\gamma'$  hardening alloys are known to harden rapidly, which in turn creates difficulties during primary (e.g. rolling and forging) and secondary (e.g. welding and machining) processing.

The  $\gamma'$ -precipitates are approximately 20–50 nm in radius after full ageing. This makes quantification using optical microscopy impossible and difficult even using scanning electron microscopy (SEM). Furthermore, it is also impossible to quantify the early stages of precipitation using tools such as transmission electron microscopy (TEM) or atom probe analysis. In addition, such tools only provide information from a very small amount of material, and no significant understanding of the volumetric content of precipitates is obtained. To date, there

\* Corresponding author.

E-mail addresses: [Sylvio.Haas@desy.de](mailto:Sylvio.Haas@desy.de) (S. Haas), [Joel.Andersson@hv.se](mailto:Joel.Andersson@hv.se) (J. Andersson), [Martin.fisk@mah.se](mailto:Martin.fisk@mah.se) (M. Fisk), [parkjs@aps.anl.gov](mailto:parkjs@aps.anl.gov) (J.-S. Park), [Ulrich.Lienert@desy.de](mailto:Ulrich.Lienert@desy.de) (U. Lienert).

<https://doi.org/10.1016/j.msea.2017.11.035>

Received 5 July 2017; Received in revised form 7 November 2017; Accepted 9 November 2017

Available online 11 November 2017

0921-5093/ © 2017 Elsevier B.V. All rights reserved.

have been no investigations of the early stages of precipitation of the  $\gamma'$ -phase in Haynes® 282®, to the authors' knowledge.

The aim of this study is to investigate the precipitation kinetics of the hardening  $\gamma'$ -phase present in Haynes® 282® using *in-situ* high-energy Small Angle X-ray Scattering (SAXS) combined with Wide Angle X-ray Scattering (WAXS). These experiments provide volumetric information concerning precipitation in terms of: number; size distribution; and inter-particle spacing during nucleation and growth [11,12]. The advantage of using high-energy X-rays (e.g. 87 keV), compared with those more commonly produced from medium-range X-ray sources (5–15 keV), is the significant increase in penetration depth. This enables the investigation of superalloys in their bulk form. In this study samples 2 mm in thickness were used (c.f. samples 50  $\mu\text{m}$  in thickness used in transmission geometries for medium-range X-ray energies [11]). *In-situ* thermo-mechanical testing was performed on these thick samples to simulate a more realistic, real-world condition. In the second part of this study, precipitation kinetics is correlated with *ex-situ* Vickers microhardness measurements. It is found from the experimental data that the hardness correlates with the square root of the product of volume fraction and mean radius of the  $\gamma'$ -precipitates.

## 2. Experimental methods

The following section describes the experimental methods used for microhardness tests and combined *in-situ* high-energy SAXS and WAXS measurements.

### 2.1. Ex-situ microhardness measurements

Test specimens made from 2 mm thick Haynes® 282® sheets, of chemical composition given in the [Supplementary information](#), were prepared by solution heat treatment at 1120 °C for 30 min. These were used for heat treatment experiments and Vickers microhardness testing using a load of 200 g for 15 s. Heat treatment experiments were carried out at 12 levels within the temperature range 600–1000 °C (600, 650, 700, 750, 775, 800, 825, 850, 875, 900, 950 and 1000 °C) for seven dwell times within the range 1–240 min (1, 5, 10, 30, 60, 120 and 240 min). The heat treatments were performed in a small lab furnace that enabled rapid heating after the specimen was inserted into the oven. The ageing time commenced when the temperature reached the ageing temperature. The temperature was measured using a type-K thermocouple attached to the specimen. To avoid the effect of grain boundaries on the results of Vickers testing, each specimen was lightly etched electrolytically at 4 V using oxalic acids. Three hardness indentations were made on each specimen for the given ageing time and temperature.

### 2.2. In-situ SAXS and WAXS measurements

A combined high-energy SAXS and WAXS experiment was performed at the Advanced Photon Source (APS), Argonne National Laboratory, USA. Haynes® 282® sheet material of thickness 2 mm, delivered in mill annealed condition (1120 °C for 30 min and slowly cooled to room temperature), was used in this study, [Fig. 1](#). The specimens from the sheet were prepared using water jet machining, which is assumed not to induce any significant heating during cutting. The samples were first solution heat treated at 1010 °C for 2 h in a vacuum furnace followed by convection cooling using argon to minimize the volume fraction of the hardening phase and to stabilize the carbides in the initial state.

Two Haynes® 282® samples were aged *in-situ* for 1 h at 760 °C and 820 °C. The experiments were carried out at beamline 1-ID-E at the APS [13] using an X-ray energy of 87 keV. The beam was vertically focused using refractive lenses, such that the focus was at the SAXS detector. The beam was horizontally defined using slits. The beam size at the sample position was approximately  $300 \times 150 \mu\text{m}^2$  (h  $\times$  v). Each

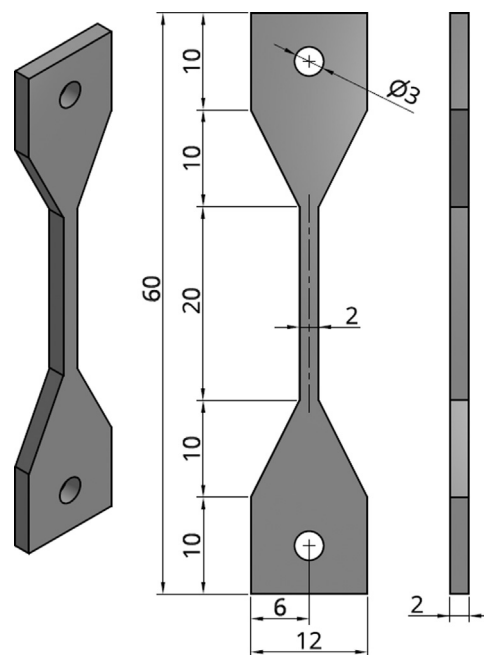


Fig. 1. Sample geometry of specimen used in SAXS/WAXS experiment.

specimen was surrounded by an infrared radiation furnace capable of heating to 1200 °C at a heating rate of 120 °C s<sup>-1</sup>. A rapid heating rate is important as it reduces pre-precipitation. The sample temperature was measured with a type-K thermocouple spot-welded onto the sample. The WAXS pattern was recorded with the Hydra setup consisting of four GE flat panel detectors [14] at a sample to detector distance of 2.63 m with an exposure time of 0.3 s. The SAXS pattern was recorded using a PIXIRAD CdTe photon counting detector [15], with a nominal pixel size of 60  $\mu\text{m}$  in a hexagonal arrangement and an exposure time of 2 s. The distance between the sample and the detector was 6.56 m. The primary beam was blocked by a 300  $\mu\text{m}$  wide tungsten beam stop in front of the SAXS detector. The primary flux and the transmitted beam intensity were measured using ionization chambers before and after the sample, respectively.

Cerium oxide and silver behenate were used to determine detector parameters for WAXS and SAXS respectively. With these detector parameters, the magnitude of the scattering vector,  $q$ , covered by the respective area detectors could be determined. A pre-calibrated glassy-carbon sample of thickness 3 mm was used to scale the SAXS intensities to differential scattering cross section (cm<sup>-1</sup>).

## 3. Results and discussion

The Vickers microhardness measurements are given in [Section 3.1](#), followed by a WAXS pattern analysis to determine the crystallographic phases and domain sizes. The phases identified by WAXS were the matrix  $\gamma$ -phase, the precipitate  $\gamma'$ -phase, primary metallic carbides MC, and secondary metallic carbides M<sub>23</sub>C<sub>6</sub>/M<sub>6</sub>C. Precipitate characterization is described in [Sections 3.3 and 3.4](#) for SAXS and WAXS, respectively. In [Section 3.5](#) the change in microhardness caused by the ageing process is compared and correlated with the findings from the quantitative SAXS analysis.

### 3.1. Vickers microhardness

[Fig. 2](#) shows Vickers microhardness data. [Fig. 2a](#)) shows the measured hardness as a function of temperature and ageing time. [Fig. 2b](#)) shows the variation in microhardness with ageing time for five temperatures (750, 775, 800, 825 and 850 °C). The figures indicate that peak hardness is achieved when the material is aged at 825 °C, with

Download English Version:

<https://daneshyari.com/en/article/7974232>

Download Persian Version:

<https://daneshyari.com/article/7974232>

[Daneshyari.com](https://daneshyari.com)